16th World Conference on Earthquake Engineering, 16WCEE 2017
Santiago Chile, January 9th to 13th 2017
Paper N° 1478
Registration Code: S-C1462777235

3D PHYSICS-BASED EARTHQUAKE SCENARIOS IN ISTANBUL FOR SEISMIC RISK ASSESSMENT

R. Paolucci(1), I. Mazzieri(2), A.G. Özcebe(3), C. Smerzini(4), M. Stupazzini(5), M. Infantino(6)

(1) *Department of Civil and Environmental Engineering, Politecnico di Milano, Italy, roberto.paolucci@polimi.it*
(2) *Laboratory for Modeling and Scientific Computing, Department of Mathematics, Politecnico di Milano, Italy, ilario.mazzieri@polimi.it*
(3) *Department of Civil and Environmental Engineering, Politecnico di Milano, Italy, aliguney.ozcebe@polimi.it*
(4) *Department of Civil and Environmental Engineering, Politecnico di Milano, Italy, chiara.smerzini@polimi.it*
(5) *Munich RE, Germany, MStupazzini@munichre.com*
(6) *MSc student, Politecnico di Milano, maria.infantino@mail.polimi.it*

Abstract

In the framework of a research cooperation between Politecnico di Milano, Italy, and Munich Re, Germany, 3D physics-based numerical simulations are carried out, considering possible realizations of a future earthquake of magnitude ranging from 7 to 7.4 along the North Anatolian fault segment facing Istanbul across the Marmara Sea. Simulations are carried out using the spectral element code SPEED (http://speed.mox.polimi.it), after construction of a numerical mesh consisting of 2.257.482 hexahedral elements of spectral degree 4, ending up with a total of 475.048.329 degrees of freedom, to cover a frequency range up to 1.5 Hz. Due to the huge dimensions of the numerical model, simulations were carried out on the supercomputer facilities available at CINECA, Italy (www.cineca.it), up to a total of about 50 scenarios, differentiated in terms of earthquake magnitude and the kinematic slip distribution. The geological setup was constructed based on different seismic microzonation and site characterization studies available in Istanbul.

Numerical results were obtained in terms of broadband ground shaking maps (0-25 Hz), referring to a region including the wide urban area of Istanbul and surroundings, for a total horizontal extension of the model of 165 x 100 km^2, down to 30 km depth. A novel approach to construct broadband accelerograms was devised, consisting of the following steps: 1) training of an artificial neural network (ANN) to correlate the simulated long period spectral ordinates with the short period ones, using a digital strong motion records database; 2) application of the ANN to estimate the short period spectral ordinates, based on the long period results of the numerical simulations; 3) application of an iterative frequency scaling procedure, with no phase change, for the simulated accelerograms to match the broadband response spectra.

The effects of different fault slip models and earthquake magnitude are tested, in order to identify the contribution to seismic hazard of different earthquake scenarios, as a function of the position of the ruptured segment along the fault, as well as the onset of possible forward directivity conditions. These numerical earthquake scenarios are the basis to construct an enhanced probabilistic/deterministic approach to seismic hazard assessment, illustrated in a companion paper submitted to the 16WCEE conference (Stupazzini et al., “PSHAe (Probabilistic Seismic Hazard enhanced): the case of Istanbul”).

Keywords: physics-based earthquake scenario; high-performance computing in elastodynamics; reinsurance policy in seismic risk mitigation

1. Introduction

In recent years, stimulated by the increasing availability of computational resources, physics-based numerical simulations of earthquake ground motion including a full 3D seismic wave propagation model from the source to the site, have gained an increasing attention worldwide (see e.g. [1-4]). The deterministic numerical approach allows one to model within a single computational domain all factors that affect earthquake ground motion, i.e.: the features of the seismic fault rupture, the propagation path in heterogeneous Earth media, directivity of seismic waves, complex site effects due to localized topographic and geologic irregularities, variability/specificity of soil properties at a regional and local scale. For this reason, they are expected to become, in near future, the most promising tool to generate ground shaking scenarios from future realistic earthquakes and to promote an advanced characterization of seismic hazard.

The most appealing features of the 3D numerical approach are: (i) modelling of the full wavefield from the extended fault rupture to the site of interest; (ii) description of the 3D variability of the dynamic properties of soils, having an impact on the spatial variability of ground motion; (iii) modelling of complex interaction of source effects (directivity, focal mechanism, etc..) and localized soil irregularities; (iv) possibility to generate realistic scenarios from future earthquakes of concern for the seismic hazard at the site. On the other hand, the main drawbacks of such an approach are: (i) frequency limitation of deterministic simulations, hardly larger than 2-3 Hz approximately; (ii) computational cost; (iii) level of detail of input geological and geotechnical data.

In the perspective of promoting tools for an advanced seismic hazard characterization, Munich RE funded a research activity with Politecnico di Milano, having a twofold objective: on one side, the release of a certified computer code to execute numerical simulations of seismic wave propagation in complex large-scale models using high-performance computing architectures, and, on the other side, the development of an advanced integrated probabilistic/deterministic procedure for seismic hazard assessment in large urban areas, making use of Physics-Based ground shaking Scenarios, referred to hereinafter as PBS, obtained by 3D numerical modelling.

The main scope of this paper is to present the 3D physics-based ground shaking scenarios generated in the Istanbul area, selected as pilot case study in the frame of this project, for the application of the integrated probabilistic/deterministic seismic risk assessment approach. A companion paper submitted to the 16WCEE conference (Stupazzini et al., "PSHAe (Probabilistic Seismic Hazard enhanced): the case of Istanbul") focuses on the presentation of such an approach.

The area of Istanbul has been selected as one of the areas with the highest seismic risk worldwide. A set of deterministic ground shaking scenarios, generated by the seismic rupture of the North Anatolian Fault (NAF) segment facing Istanbul across the Marmara Sea, with magnitude M_W ranging from 7 to 7.4 and variable kinematic slip distribution, has been simulated through a 3D numerical model by spectral elements for the area of Istanbul. Numerical simulations are carried out using an innovative high-performance computer code called SPEED ([5]) based on the Discontinuous Galerkin Spectral Elements Method (DGSEM), which is particularly useful in tackling multi-scale seismic wave propagation problems in highly heterogeneous media. Relying on a novel approach for generating broadband ground motions, based on Artificial Neural Networks (ANNs), PBSs are provided in the whole frequency range of interest of engineering applications.

After showing an overview of the seismotectonic context of the Istanbul area and the main motivation behind the selection of this case study, the computational approach and relevant tools will be presented. Then, the main features of the 3D numerical model will be illustrated with emphasis on the geologic, topography and bathymetry setup. An overview of the main results of the numerical simulations will be shown to shed light on the main factors affecting seismic hazard estimation, such as directivity effects.

2. Why the Istanbul area?

The Istanbul-Marmara region of northwestern Turkey with a population of more than 15 millions, faces an high probability (62 +/- 15 %, ref [6]) for the occurrence of an earthquake of magnitude 7 or more. The cause can be found in the seismic gap beneath the Sea of Marmara, some five miles west of Istanbul: since the disastrous 1939

Erzincan earthquake (Magnitude 7.9), major earthquakes have occurred along the North Anatolian Fault (NAF) in a roughly domino-like fashion, breaking sequentially from east to west. The chain of earthquakes along the North Anatolian fault presents a gap at south of Istanbul as shown in Fig. 1 (from [7]).

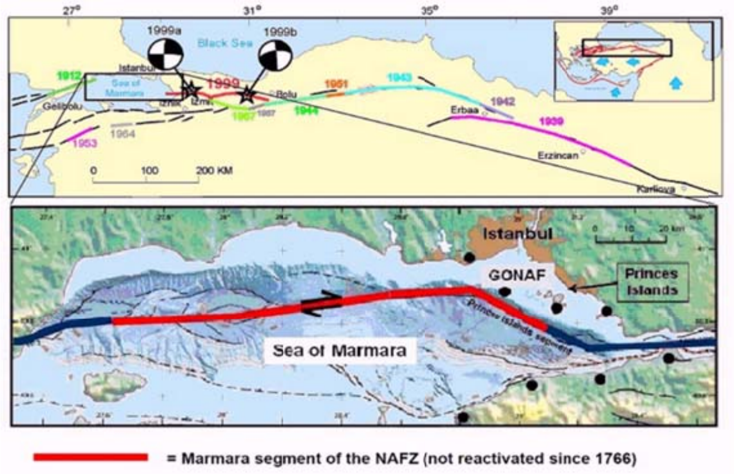

Fig. 1 – Top panel: sites and the length of the fractures of the NFA; bottom panel: seismic gap at the Marmara sea, the red segment of the NAFZ has been not reactivated since 1766. From [7].

Separate groups of authors have advocated different models to explain the origin of this seismic gap because of poor seismic coverage and insufficient use of available earthquake data. Each model has significant different implications for the seismic hazard at Istanbul: depending on the model, the Marmara seismic gap could be ruptured either by a single large earthquake or multiple smaller earthquakes with large differences in the resulting ground shaking and damage.

The expected earthquakes in this region represent an extreme danger for the Turkish megacity. Istanbul is, in fact, one of the world´s most populous cities and many buildings or constructions are very old and not built to the highest modern standards compared to other seismic areas of the world. A big earthquake could cause many victims and economics damages. Because the considerable sum insured in the Istanbul area and the high seismic risk, Munich Re is very interested in a detailed study of this case.

3. The computational approach

This section aims at illustrating the computational approach which has been used to generate the 3D PBSs in the Istanbul area. This involves three main tools: (1) the computer code SPEED running on parallel computer architectures; (ii) a pre-processing tool, i.e. a rupture generator, to produce a set of kinematic slip models along a given fault within a prescribed magnitude; (iii) a post-processing tool to generate broadband (BB) ground motions starting from the results of SPEED, applicable only to the low frequency range.

3.1 SPEED: Spectral Elements in Elastodynamics with Discontinous Galerkin

The open-source software package SPEED (*SPectral Element in Elastodynamics with Discontinuous Galerkin*: http://speed.mox.polimi.it/) is designed for the simulation of large-scale seismic wave propagation problems including the coupled effects of a seismic fault rupture, the propagation path through Earth's layers, localized geological irregularities, such as alluvial basins, and soil-structure interaction problems (see e.g. [5]). Based on a discontinuous version of the classical spectral element (SE) method, as explained in [8], SPEED is naturally oriented to solve multi-scale numerical problems, allowing one to use non-conforming meshes (*h*-adaptivity) and different polynomial approximation degrees (*N*-adaptivity) in the numerical model. SPEED is designed for multi-core computers or large clusters (e.g., Fermi BlueGene/Q at CINECA), taking advantage of the hybrid MPI-OpenMP parallel programming.

3.2 Pre-processing tool: automatic generation of seismic slip distributions

A pre-processing tool has been devised, in order to automatically construct N physically constrained slip distributions for a given fault and a given earthquake magnitude, taking into account joint probability distributions of the main kinematic parameters. This is necessary to control that the resulting scenario variability will be not affected by systematic bias in the input parameters. Two kinematic source rupture generators have been tested: Herrero and Bernard (1994) (see [9]), referred to as HB94 model, and Crempien and Archuleta (2015) (see [10]), referred to as CA15 model. While for the latter we refer the reader to the relevant publication (the code is available on the SCEC Broadband Platform), for the former some implementation details are given below.

Given a fault type (e.g., reverse=R, normal=N or strike slip=SS) and a target magnitude M (e.g., 7 or 7.4), a Matlab routine computes suitable input parameters for the generation of a slip distribution according a k^2 Herrero model. In particular the fault length (L), the fault width (W), the maximum displacement (MD) and the average displacement (AD) of the slip distribution are computed using the well-known relations by Wells & Coppersmith (1994) (ref. [11]). In addition the hypocenter position (Hypo) and the asperity locations (AL) are calculated run-time randomly, using a Gaussian distribution for the former (with mean μ = 10 km depth and variance σ^2 = 2 km) and uniform distribution for the latter. After this process, the slip distribution is randomized in a suitable way to radiate seismic energy in a broadband frequency range, limited by the resolution of the numerical mesh.

3.3 Post-processing tool: broadband ground motions based on Artificial Neural Network

To overcome the frequency limitation of the numerical simulations, a novel approach is proposed to generate broadband ground motions (referred to as BB hereinafter), with realistic features in the entire frequency range of interest for engineering applications (say between 0 and 25 Hz), using Artificial Neural Networks (ANN) combined with spectral matching techniques.

The main steps of this approach can be summarized as follows (see Fig. 2):

(1) Training of an ANN based on recorded earthquake ground motions (namely, SIMBAD database, presented in [12]) to predict M response spectral ordinates at short period (SP, $T \leq T^*$, being T the vibration period and T* a suitably chosen corner period) from N spectral ordinates at long period (LP, $T > T^*$);

(2) For each site of interest and for a given scenario, the trained ANN is applied to estimate the SP response spectral ordinates, taking as input the LP spectral ordinates computed from SPEED ground motions. Hence, a target broadband response spectrum is constructed, combining the LP ordinates produced by SPEED with the SP ordinates predicted by the ANN;

(3) Application of spectral matching techniques to the LP time histories produced by SPEED to obtain BB ground motions fitting the target spectrum obtained at previous point.

To design the network, the following assumptions have been made: (i) a two-layer feed-forward (2LFF) neural network with 30 sigmoid hidden neurons and a linear output neuron was trained with the Levenberg-Marquaredt algorithm, using the neural network fitting tools (*nftool*) implemented in Matlab; (ii) inputs are N=21 ground motion parameters, specifically, Log10[SA(Tj), PGV, PGD], where SA is the pseudo-acceleration response spectral ordinates at period Tj, ranging from 0.8 s to 5 s, PGV is the Peak Ground Velocity and PGD is the Peak Ground Displacement; (iii) outputs are M=10 ground motion parameters, specifically, Log10[SA(T_k)], at periods T_k = 0 (PGA = Peak Ground Acceleration), 0.05, 0.1:0.1:0.7, 0.75 s. Note that T*=0.75 s in this study and its choice is related to the frequency limit of the numerical simulations.

For the application presented in this work, we have limited our attention to the construction of the broadband target response spectrum (step 1 and 2 of the procedure). In this context, training of the ANN has been performed using the geometric mean of the horizontal components; however, the procedure can be extended by training different ANN separately for the three components of motion. Furthermore, to have better constrained predictions for large magnitude events, as the ones simulated by SPEED, the original SIMBAD database has been enlarged before training, including a set of 22 records from the 1999 Chi-Chi (M_W=7.6) and 1999 Kocaeli (M_W =7.35) earthquakes.

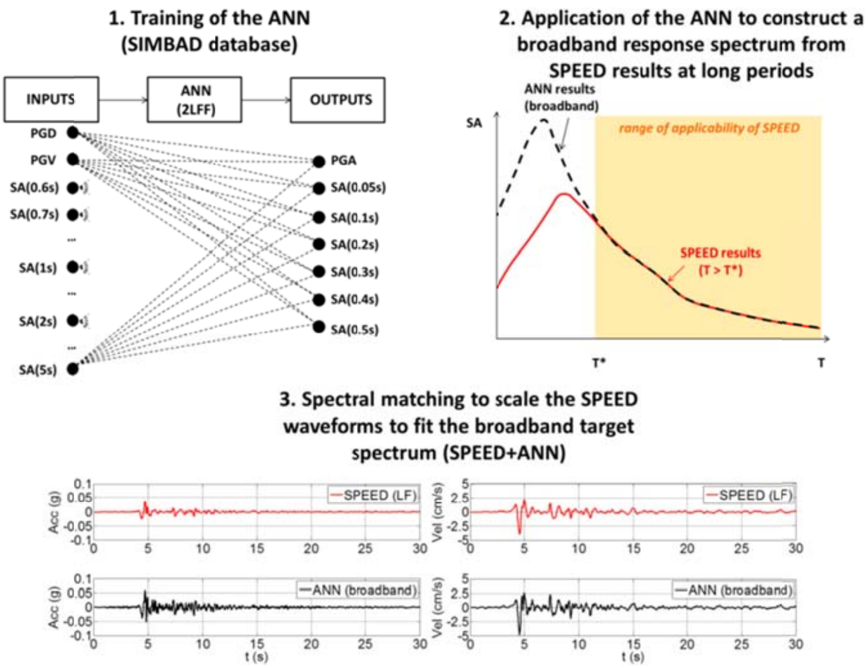

Fig. 2 – Sketch of the procedure to generate BB ground motions from SPEED scenarios.

4. Setup of the 3D numerical model

The 3D numerical model was constructed by combining the following features: (i) the topography and bathymetry model; (ii) the kinematic seismic fault model (see procedure described in Section 3.2); (iii) the 3D velocity model. In the following details of these aspects will be provided and, finally, the resulting hexahedral mesh will be described.

4.1 Topography and bathymetry

For the elevation model, freely-available digital elevation dataset of CGIAR-CSI for the *Tracia* region has been extracted and downloaded from the website http://www.cgiar-csi.org (with a precision of roughly 70 x 90 m, for east-west and north-south directions around Istanbul city), while the bathymetry model has been derived from the MATLAB digitalization of the map proposed by Özsoy et al. 2000 [13]. Hence elevation and bathymetry models, both in a numerical format, have been assembled together in MATLAB environment obtaining the top surface of the computational domain, as illustrated in Fig. 3.

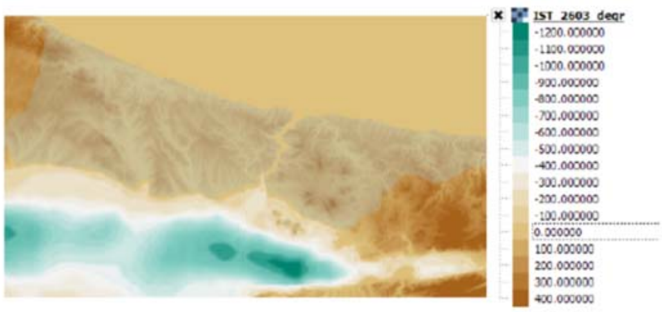

Fig. 3 – Combined digital elevation/bathymetry model.

4.2 Seismic fault

The seismic fault considered consists of the Central Marmara Basin (CMB) and North Boundary Fault (NBF), part of the NAF, located about 20-30 km south-west and south of Istanbul respectively, as shown in Fig. 4. The source is a vertical segmented fault, consisting of three main segments with different strike angles. The total length of the fault is around 98 km, capable of producing a M_W 7.4 event. The geometric parameters of the NBF, as implemented in the numerical model, are reported in Table 1.

Table 1 – Geometric parameters of the North Boundary Fault (NBF).

Segment	Strike (deg)	Dip (deg)	Rake (deg)	L_{max} (m)	W_{max} (m)	Fault Origin* (Lon [°N];Lat [°E])	Top depth (m)
1	81.5	90	0	58000	30000	28.12;40.81	836.5
2	99.6	90	0	10400	30000	28.79;40.88	655.7
3	119.3	90	0	30000	30000	28.91;40.86	543.8

**Fault Origin is defined as the point of the fault at zero strike and zero dip*

4.3 Soil characterization (3D velocity model)

In order to define the 3D soil model a three-step procedure has been adopted according to the geotechnical site characterization provided by Özgül (2011) (see [14]). First the digitalization of the maps presented by Özgül (2011) has been performed to obtain the map of $V_{S,30}$ and rock/soil information for the whole Istanbul region. Second, by making use of three sets of data, namely $V_{S,30}$, rock/soil map and slope information (extrapolated by QGIS, www.qgis.org), different site classes have been assigned ranging from $V_{S,30}$ = 250 m/s to $V_{S,30}$ = 1350 m/s, see colored map in Fig. 4 (left). Third, the model has been improved for the Avcılar zone, characterized by very soft sediments, where significant soil effects occurred during the 1999 Kocaeli Earthquake (see [15]), by reassigning the soil class as the softest. Finally, six homogeneous V_S profiles have been considered in the first layer (0 to 5 km depth) with a prescribed gradient, as shown in Fig. 4 (right). The properties of the underlying bedrock layers (depth > 5 km) have been obtained by the interpretation of seismic profiles presented in Cotton et al. (2006) (see [15]) and Gurbuz et al. (2000) (see [17]). The quality factor Q is derived directly by the V_S values and is assumed to be proportional to frequency as $Q = Q_0 \cdot f$, with Q_0 set for the target value $Q = V_S/10$ to be obtained at f = 1 Hz. The 3D velocity model is summarized in the table on the right hand side of Fig. 5.

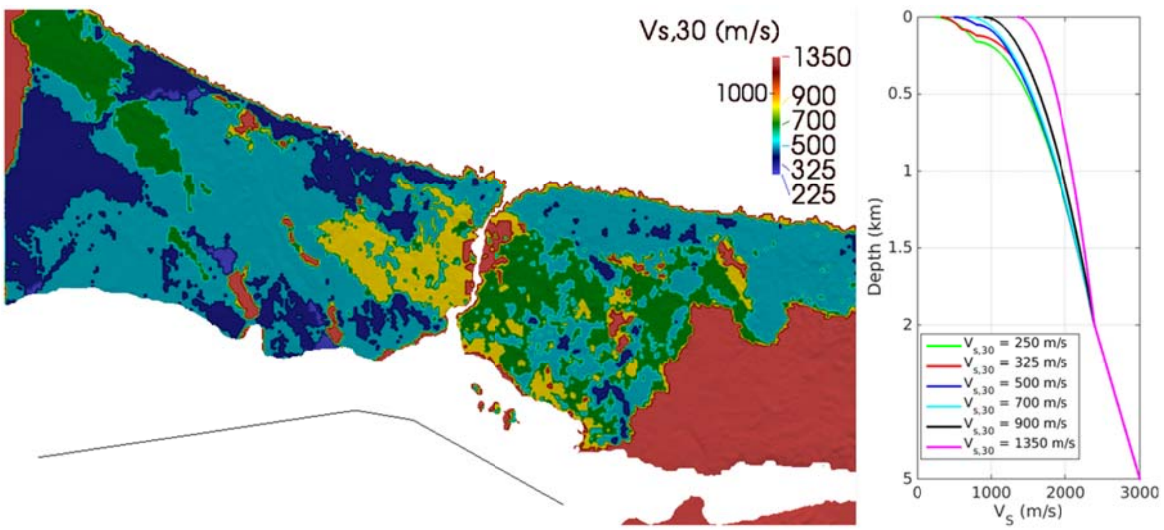

Fig. 4 - $V_{S,30}$ classes defined according to Özgül, 2011 (left). V_S, profiles adopted in the present work for the six soil classes considered in the first layer (0 to 5 km depth) of the computational domain (see also Fig. 5).

4.4 Mesh

The computational domain, which extends over an area of 165x100x30 km^3 down to 30 km depth (see Fig. 5), has been built combining all the information previously described. Considering a rule of thumb of 5 grid points per minimum wavelength for non-dispersive wave propagation in heterogeneous media by the SE approach (see [7]), and considering a maximum frequency f_{max} = 1.5 Hz, the model consists of 2,257,482 hexahedral elements, resulting in approximately 475 million of degrees of freedom, using a fourth order polynomial approximation degree. The conforming mesh has a size varying from a minimum of 180 m, on the top surface, up to 600 m at 2 km depth and reaching 1800 m in the underlying layers.

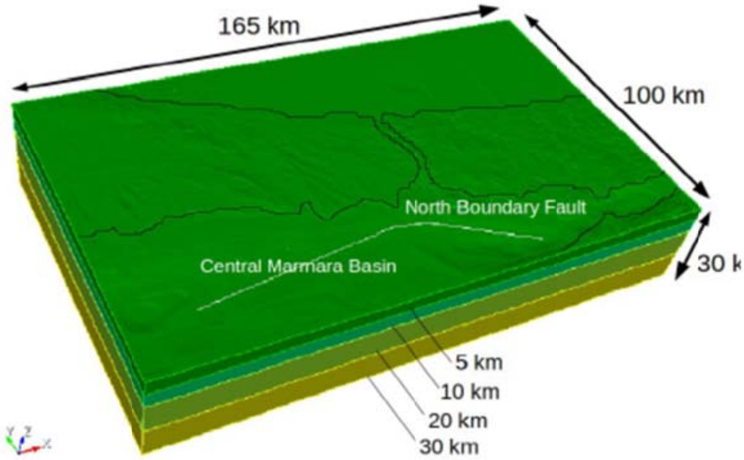

Horizontally stratified crustal model

Depth (km)	V_S (m/s)	(-)
0-5	Fig. 4 (right)	Vs/10
5-10	3490	350
10-20	3500	400

Fig. 5 - Computational domain of the Istanbul region adopted in the present work. Fault system (CMB and NBF) included in the domain as well as topography and bathymetry model.

5. Summary of simulated scenarios

A total of 51 scenarios were simulated by varying the magnitude, from 7.0 up to 7.4, the kinematic slip distribution, the hypocenter location and the location of the rupture area. The simulations were performed on the Fermi cluster located at CINECA, Italy (http://www.cineca.it/en/content/fermi-bgq). Each simulation takes around 14 hours on 2048 cores. A summary of the seismic scenarios, grouped for magnitude and source, is given in Table 2. Note that for each scenario, the rupture velocity is fixed to $0.85 \cdot V_S$, to avoid supershear effects, the rise time is randomized around a mean value of 0.7 s for the HB94 source, while follows the built-in scheme for the CA15 model, and the source time function is a simplified smoothed Heaviside function. For each simulation a time step equal to 0.001 s has been chosen for the time marching scheme and a total observation time T = 60 s has been considered.

Table 2 – Simulated scenarios grouped for magnitude and source

Source / M_W	7.0 (57x12 km^2)	7.2 (84x15 km^2)	7.4 (96x15 km^2)
HB94	20	10	6
CA15	4	7	4

6. Overview of numerical results

In this section some salient features of the simulated scenarios are presented, focusing on the time histories at selected locations, the spatial variability of ground motion in the whole frequency range of interest (0-25 Hz), the effect of the source model (HB94 vs CA15) and the analysis of forward directivity effects.

First, Fig. 6 shows the simulated velocity time histories for a M_W7.0 scenario at some strategic sites in the Istanbul area, superimposed on the PGV map, for the Horizontal (x, y) and Vertical (z) components. Synthetics are processed with an acausal Butterwort filter with high and low pass frequency equal to 0.05 Hz and 1.5 Hz, respectively, the latter being related to the frequency limit of the numerical model.

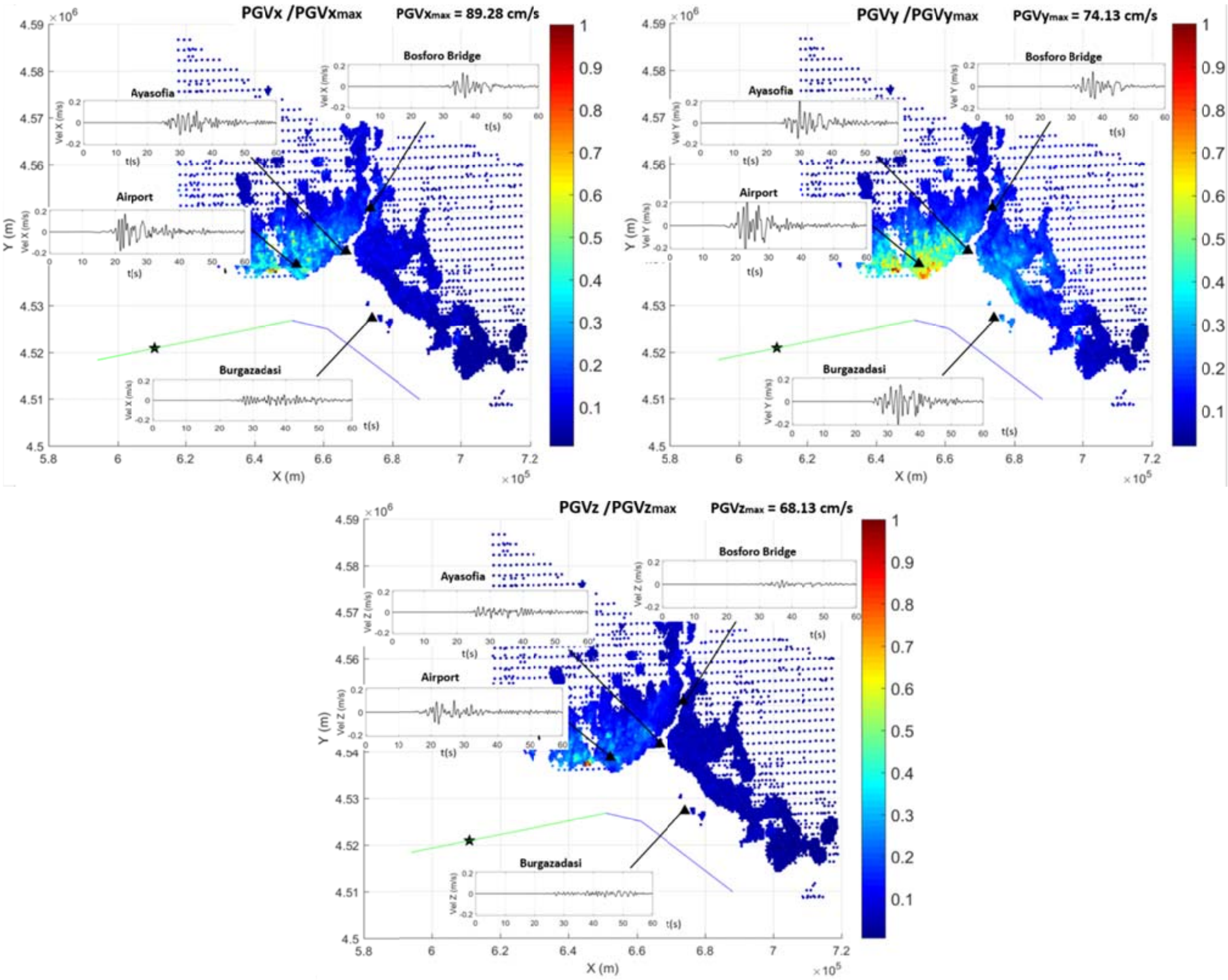

Fig. 6 - Velocity time histories superimposed on the PGV map for the vertical (bottom panel) and the two horizontal (top panels) components of a scenario of magnitude 7.0 (ID 509) for some strategic sites (Ayasofia (*ing.* Haghia Sophia), Airport, Bosforo (*ing.* Bosphorus) Bridge and Burgaz Adası). The scheme of the fault, epicenter (black star) and the active segment (green) of the considered scenario are also shown.

To illustrate the advantage of the ANN-based approach proposed in this study to generate BB ground shaking scenarios, we show in Fig. 7, for the same scenario of magnitude 7.0 as considered in Fig. 6, maps of response spectral acceleration (PSA) at different vibration periods, ranging from 0 s (PGA, top left) to 5.0 s ($PSA_{5.0s}$, bottom right). It is worth remarking that this novel approach allows one to preserve the full spatial correlation of ground motion and to incorporate important physical features, such as directivity effects and 3D complex site effects, also at short periods (i.e. at T < 1.0 s, see top panels of Fig. 7), as inherited from the low frequency spectral ordinates.

Furthermore, as an illustrative example of the effect of the fault slip model, we compare in Fig. 8 the PGV maps obtained for two scenarios having the same magnitude (M_W =7.0), position of hypocenter and causative rupture fault area, but being generated with the two kinematic rupture generator models, i.e., HB94 (left) vs CA15 (right). We can note that the slip distribution is rather different: in the HB94 model it is more coherent with higher value of maximum slip (bottom left panel), while in the CA15 model it is much more scattered with a lower value of maximum slip (bottom right panel). The larger coherence of the HB94 slip model turns out to produce higher values of peak ground velocity over a more extended area (as indicated by the map on the top panels).

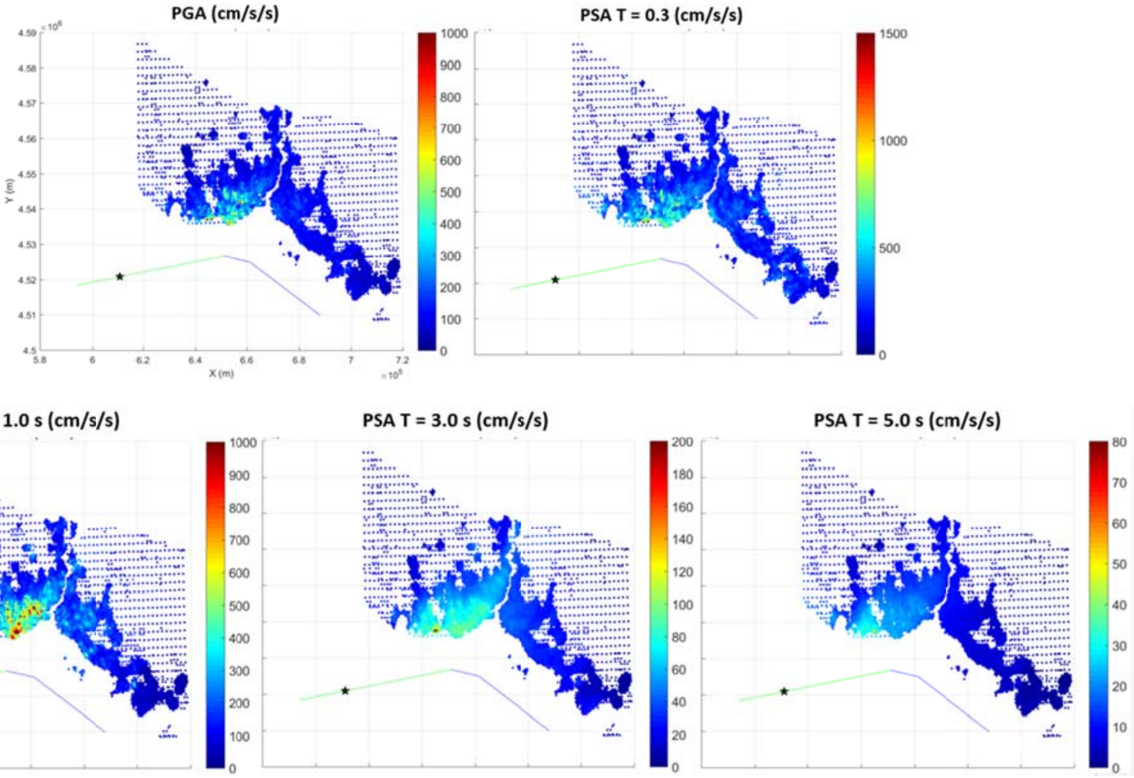

Fig. 7 - From left top to right bottom: PGA, PSA at 0.3 s, PSA at 1s, PSA at 3.0 s, PSA at 5.0 s maps obtained by SPEED + ANN for a scenario of M_W 7.0 (ID 509). The active fault is highlighted in green and epicenter position is represented by a black star.

Finally, the analysis of the set of PBSs as a function of earthquake magnitude (7.0 vs 7.2 vs 7.4) has led to the identification of interesting forward directivity conditions. Contrarily to case of an earthquake of M_W=7.0, when an earthquake of $M_W \geq 7.2$ occurs, the rupture will always involve the three segments of the NFA. In these cases Istanbul will be always interested by forward directivity effects, owing to its unlucky position with respect to the propagation of rupture, leading to a strong amplification of ground motion. On the other side, for events of M_W 7.0, it is possible distinguish between forward, neutral and backward directivity depending on the combination of the relative position of the hypocenter and slip distribution. These directivity effects, specific for large magnitude events ($M_W \geq 7.2$), cannot be taken into account by the standard GMPEs, which are poorly constrained in the near-source region of large earthquakes. Concerning this, Fig. 9 shows the comparison between the mean residuals, in terms of PGV, of the set of simulated scenarios of M_W 7.0 (left) and that of M_W 7.2 (right) with respect to two GMPEs (top: CHYO08 = Chiou and Youngs, 2008, ref. [18]; bottom: CAEA14 = Cauzzi et al. (2014) – ref. [19]). At each observation point (*x, y*) of the model, the mean residuals for a given magnitude M_W is computed as follows:

$$R(x, y, M_W) = \frac{1}{N}\sum_{i=1}^{N} log_{10}\frac{PBS(x,y,M_W)_i}{GMPE(x,y,M_W)} \tag{1}$$

where *N* is the number of simulations for the prescribed magnitude, PBS refers to the intensity measure (e.g. PGV) predicted by SPEED while GMPE to that predicted by the selected empirical attenuation law. It is apparent that for the simulation set with M_W =7.2, the residuals are always positive, i.e., the values of ground motions simulated are higher than that predicted by GMPEs for all sites while for the set of M_W 7.0 the residuals are in the range of [- 0.2, 0.2].

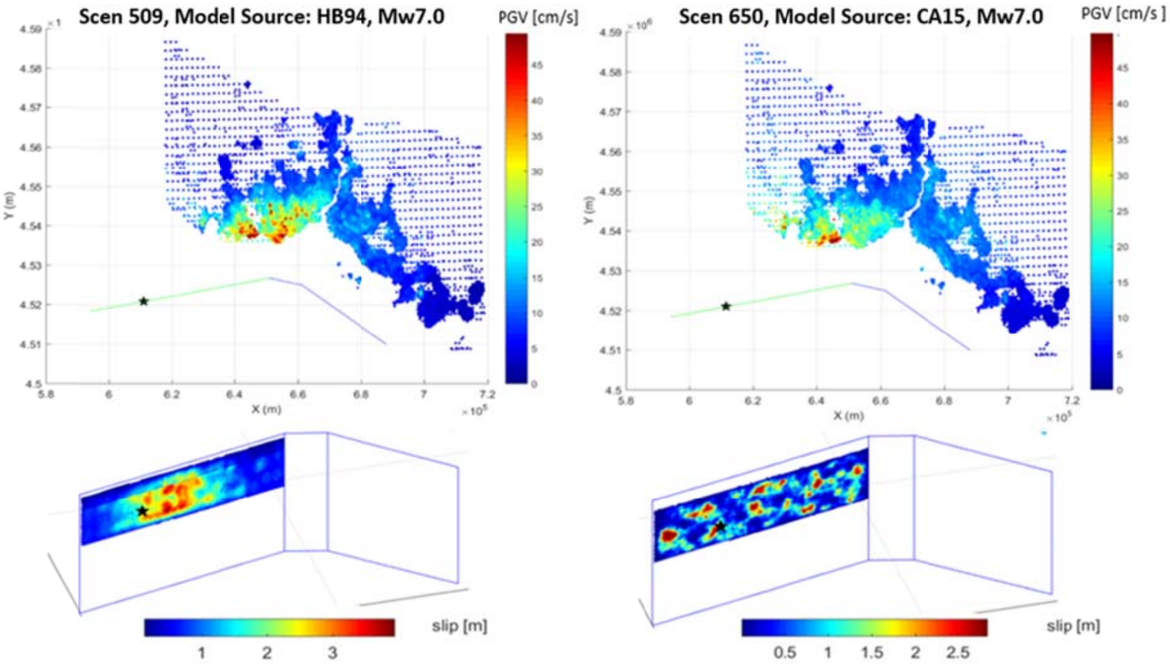

Fig. 8 – Top: PGV maps obtained by SPEED for two scenarios of M_W 7.0 generated with the HB94 (left panel) and CA15 source model (right panel). The ruptured fault area is highlighted in green and the epicenter position is represented by a black star. Bottom: slip distribution considered for the scenarios.

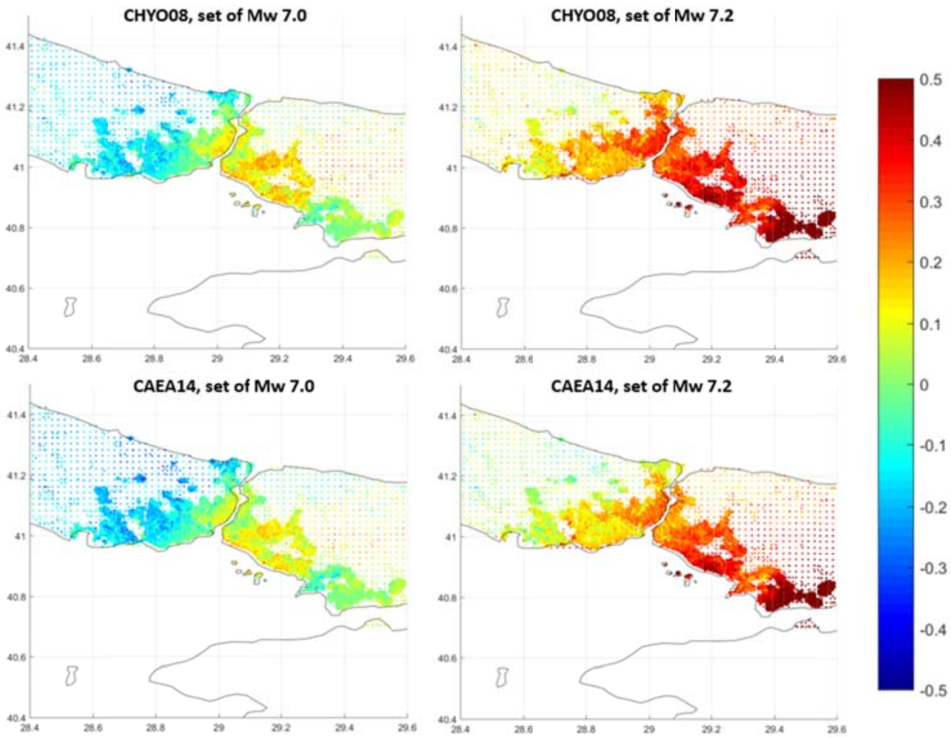

Fig. 9 – Maps of mean residuals, *R* (see Eq. (1)), in terms of PGV, considering all scenarios (only HB94 source model) with a prescribed value of magnitude, namely, M_W =7.0 on the left panels and M_W =7.2 on the rigth panels. Residuals are computed with respect to both CHYO08 (top panels) and CAEA14 (bottom panels).

7. Concluding Remarks

In this paper, 3D physics-based numerical simulations of earthquake ground motion in the area of Istanbul, Turkey, have been presented. To perform these simulations, a large-scale 3D spectral element model up to maximum frequencies of 1.5 Hz has been constructed, combining the following features: (i) the topography and bathymetry; (ii) the kinematic seismic fault model; (iii) the 3D velocity model, as derived from different seismic microzonation and site characterization studies available for the Istanbul region. Using this computational model, a wide set of ground shaking scenarios (around 50) has been generated, considering possible realizations of a future characteristic earthquake of magnitude in the range 7.0-7.4, originating from the North Anatolian Fault segment facing Istanbul across the Marmara Sea. This is the fault segment associated with a clear seismic gap and, therefore, with a high probability of producing a large earthquake ($M_W \geq 7.0$) in the next future. The scenarios were defined by varying the magnitude, the slip distribution according to two kinematic source models (HB94 and CA15), the position of the hypocenter and the location of the broken fault area. Numerical simulations were carried out on parallel computers using the open-source code SPEED, based on the Discontinous Galerkin Spectral Element Method.

To overcome the frequency limit of the numerical simulations, a novel approach based on Artificial Neutral Networks (ANN) has been applied to generate broadband ground shaking scenarios, usable over the entire frequency range of interest (0-25 Hz) for seismic risk applications. This approach turns out to be particularly interesting because it allows one to preserve the full spatial correlation of ground motion, as inherited from low frequency simulations, and, consequently, to incorporate important physical features, such as directivity effects and 3D complex site effects, also at short periods.

The analysis of the simulated scenarios points out that significant forward directivity effects govern seismic ground motion estimates in case of strong earthquakes, i.e., $M_W \geq 7.2$, regardless of the earthquake realization, owing to its systematic unlucky position with respect to the propagation of rupture. This may have a great impact on seismic hazard estimates, as standard GMPEs cannot account for such effects.

The numerical results presented in this paper are the basis to develop improved seismic hazard assessment studies, whose distinguishing feature is the direct incorporation of 3D deterministic numerical scenarios, with their physical spatial correlation characteristics, into the probabilistic seismic hazard assessment framework.

8. Acknowledgements

We deeply thank André Herrero and Jorge Crempien for the codes they have provided. This work has been carried out in the framework of the 2015-2017 cooperation project between Munich Re and Politecnico di Milano, with the contribution of Alexander Allmann and Martin Käser. The 3D numerical simulations were performed on FERMI cluster, at CINECA, in the framework of the ISCRA PBES4HAS project. Ilario Mazzieri has been partially funded by Fondazione Cariplo and Regione Lombardia (Project n. 2015-0182).

9. References

[1] Jones LM, Bernknopf R, Cox D, Goltz J, Hudnut K, Mileti D, Perry S, Ponti D, Porter K, Reichle M, Seligson H, Shoaf K, Treiman J, Wein A (2008): The ShakeOut scenario. *Technical Report USGS-R1150*, U.S. Geological Survey and California Geological Survey.

[2] Graves RW, Jordan T, Callaghan S, Deelman E, Field E, Juve G, Kesselman C, Maechling P, Mehta G, Milner K, Okaya D, Small P, Vahi K (2010): CyberShake: a physics-based seismic hazard model for Southern California. *Pure and Applied Geophysics*, **168** (3–4), 367–381.

[3] Bielak J, Graves RW, Olsen KB, Taborda R, Ramirez-Guzman L, Day SM, Ely GP, Roten D, Jordan TH, Maechling PJ, Urbanic J, Cui Y, Juve G (2010): The ShakeOut earthquake scenario: verification of three simulation sets. *Geophysical Journal International*, **180**, 375–404.

[4] Paolucci R, Mazzieri I, Smerzini C, Stupazzini M (2014): Physics-based earthquake ground shaking scenarios in large urban areas, in *Perspectives on European Earthquake Engineering and Seismology, Geotechnical, Geological and Earthquake Engineering*, vol. 34, chap. 10, pp. 331–359, ed. Ansal, A., Springer

[5] Mazzieri I, Stupazzini M, Guidotti R, Smerzini C (2013): SPEED: SPectral Elements in Elastodynamics with Discontinuous Galerkin: a non-conforming approach for 3D multi-scale problems, *International Journal for Numerical Methods in Engineering*, **95**(12), 991–1010.

[6] Parsons T, Toda S, Stein R S, Barka A and Dieterich J H (2000): Heightened odds of large earthquakes near Istanbul: An interaction-based probability calculation, *Science*, **288**, 661- 665.

[7] Bohnoff M, Martinez-Garzon P, Bulut F, Stierle E, Ben-Zion Y (2016): Maximum earthquake magnitudes along different sections of the North Anatolian fault zone, *Tectonophysics*, **674** (2016),147-165.

[8] Antonietti PF, Mazzieri I, Quarteroni A, Rapetti F (2012): Non-conforming high order approximations of the elastodynamics equation, *Computer Methods in Applied Mechanics and Engineering*, **209–212**, 212–238.

[9] Herrero A and Bernard P (1994): A kinematic self-similar rupture process for earthquakes, *Bulletin of Seismological Society of America*, **84**(4), 1216–1228.

[10] Crempien JGF, Archuleta RJ (2015): UCSB Method for Simulation of Broadband Ground Motion from Kinematic Earthquake Sources, *Seismological Research Letters*, **86** (1), 61-67.

[11] Wells LD, Coppermisth JK (1994): New Empirical Relationships among Magnitude, Rupture Length, Rupture Width, Rupture Area, and Surface Displacement, *Bulletin of the Seismological Society of America*, **84** (4), 974-1002.

[12] Smerzini C, Galasso C, Iervolino I, Paolucci R (2014): Ground motion record selection based on broadband spectral compatibility, Earthquake Spectra, **30** (4), 1427-1448.

[13] Özsoy E, Beşiktepe Ş, Latif M A (2000): Türk Boğazlar Sistemi'nin Oşinografisi, Marmara Denizi 2000 Sempozyumu, İstanbul, 11-12 November (in Turkish).

[14] Özgül N (2011). İstanbul İl Alanının jeolojisi. Yönetici Özeti. İstanbul Büyükşehir Belediyesi, Deprem ve Zemin İnceleme Müdürlüğü (in Turkish).

[15] Tezcan S S, Kaya E, Bal İ E, Özdemir Z (2002): Seismic amplification at Avcılar, Istanbul, *Engineering Structures*, **24**, 661-667.

[16] Cotton F, Scherbaum F, Bommer J J, Bangum H (2006): Criteria for selecting and adjusting ground-motion models for specific target regions: Application to Central Europe and rock sites, *Journal of Seismology*, **10**, 137-156.

[17] Gurbuz C, Aktar M, Eyidogan H, Cisternas A, Haessler H, Barka A, Ergin M, Türkelli N, Polat O, Üçer SB, Kuleli S, Baris S, Kaypak B, Bekler T, Zor E, Bicmen F, Yoruk A (2000): The seismotectonics of the Marmara region (Turkey): results from a microseismic experiment, *Tectonophysics*, **316** (1): 1-17.

[18] Chiou B S-J,Youngs R R (2008): An NGA model for the average horizontal component of peak ground motin and response spectra, *Earthquake Spectra*, **24**(1), 173-215.

[19] Cauzzi C, Faccioli E, Vanini M, Bianchini A (2014): Update predictive equations for broadband (0.01 to 10 s) horizontal response spectra and peak ground motions, based on a global dataset of digital acceleration records, *Bulletin of Earthquake Engineering,* **13**/6, 1578-612.